

Density-Matrix Algorithm for Phonon Hilbert Space Reduction in the Numerical Diagonalization of Quantum Many-Body Systems

Alexander Weiße¹, Gerhard Wellein², and Holger Fehske¹

¹ Physikalisches Institut, Universität Bayreuth, D-95440 Bayreuth

² Regionales Rechenzentrum Erlangen, Universität Erlangen, D-91058 Erlangen

Abstract. Combining density-matrix and Lanczos algorithms we propose a new optimized phonon approach for finite-cluster diagonalizations of interacting electron-phonon systems. To illustrate the efficiency and reliability of our method, we investigate the problem of bipolaron band formation in the extended Holstein Hubbard model.

1 Introduction

Considerable work is currently focused on the experimental and theoretical study of strongly coupled electron-phonon (EP) systems, triggered by the recognition that the EP interaction plays an important role in understanding the physics of novel materials such as colossal magneto-resistance manganites [1] or the very recently discovered superconducting magnesium diboride [2]. From a theoretical point of view the challenge is to describe the partly exotic properties of these materials in terms of simplified microscopic models which take into account the complex interplay of charge, spin and lattice degrees of freedom.

As a generic model for systems with competing electron-electron and electron-phonon interactions the extended Holstein Hubbard model (EHHM),

$$\mathcal{H} = -t \sum_{\langle i,j \rangle; \sigma} c_{i\sigma}^\dagger c_{j\sigma} + U \sum_i n_{i\uparrow} n_{i\downarrow} - \sum_{i,l;\sigma} f_l(i) n_{i\sigma} x_0 (b_l^\dagger + b_l) + \omega_0 \sum_i (b_i^\dagger b_i + \frac{1}{2}), \quad (1)$$

is usually considered [3,4,5], where $c_{i\sigma}^{[\dagger]}$ and $b_i^{[\dagger]}$ annihilates [creates] a spin- σ electron and a phonon at Wannier site i , respectively, and $n_{i\sigma} = c_{i\sigma}^\dagger c_{i\sigma}$. The Hamiltonian (1) consists of a kinetic term describing the electronic motion on a discrete lattice (transfer amplitudes t), an extremely screened (on-site) Coulomb repulsion (Hubbard parameter U), and a “density-displacement” type non-screened EP coupling ($\propto \kappa x_0$)

$$f_l(i) = \frac{\kappa}{(|l-i|^2 + 1)^{3/2}}, \quad x_0 = \sqrt{1/2M\omega_0}, \quad \kappa x_0 = \sqrt{\varepsilon_p \omega_0}. \quad (2)$$

Here ω_0 is the bare phonon frequency of dispersionsless optical phonons, being polarized in the direction perpendicular to the chain (1D case). Defining the polaron binding energy as $\tilde{\varepsilon}_p = (x_0^2/\omega_0) \sum_l f_l^2(0) = 1.27\varepsilon_p$, the famous Holstein Hubbard model (HHM) results by setting

$$f_l(i) = \kappa\delta_{i,l}, \quad \tilde{\varepsilon}_p \rightarrow \varepsilon_p, \quad (3)$$

i.e., with respect to the EP coupling term the EHHM represents an extension of the Fröhlich model [6] to a discrete ionic lattice or of the Holstein model [7] including longer ranged EP interactions.

Adapting the EHHM to real physical situations one is frequently faced with the difficulty that the energy scales of electrons (t , U), phonons (ω_0) and their interaction ($\tilde{\varepsilon}_p$) are of the same order of magnitude, causing analytic methods, and especially adiabatic techniques, to fail in most of these cases. Thus, at present, the most reliable results came from powerful numerical calculations, such as finite-cluster exact diagonalizations (ED) [8,9,10] or (Quantum) Monte Carlo simulations [11,12], which are usually performed on supercomputers. But even for these numerical approaches strong EP interactions are a demanding task, since they require some cut-off in the phonon Hilbert space. Starting with the work of White [13] in 1993, during the last years a class of algorithms became very popular, which based on the use of a so-called density matrix for the reduction of large Hilbert spaces to manageable dimensions.

In the present paper, we will demonstrate that finite-cluster diagonalization methods also benefit substantially from these ideas. Along this line, in the next section we introduce an optimized phonon approach for the ED of electron-phonon problems. To exemplify this technique, we analyze the formation of bipolarons in Sec. III. Our main results are summarized in Sec. IV.

2 Optimized phonon approach

Let us first resume the connection between density matrices and optimized basis states. Starting with an arbitrary normalized quantum state

$$|\psi\rangle = \sum_{r=0}^{D_r-1} \sum_{\nu=0}^{D_\nu-1} \gamma_{\nu r} |\nu\rangle |r\rangle \quad (4)$$

expressed in terms of the basis $\{|\nu\rangle|r\rangle\}$ of the direct product space $H = H_\nu \otimes H_r$, we wish to reduce the dimension D_ν of the space H_ν by introducing a new basis,

$$|\tilde{\nu}\rangle = \sum_{\nu=0}^{D_\nu-1} \alpha_{\tilde{\nu}\nu} |\nu\rangle, \quad (5)$$

with $\tilde{\nu} = 0 \dots (D_{\tilde{\nu}} - 1)$ and $D_{\tilde{\nu}} < D_{\nu}$. The projection of $|\psi\rangle$ onto the corresponding subspace $\tilde{H} = H_{\tilde{\nu}} \otimes H_r \subset H$ is given by

$$\begin{aligned} |\tilde{\psi}\rangle &= \sum_{r=0}^{D_r-1} \sum_{\tilde{\nu}=0}^{D_{\tilde{\nu}}-1} \sum_{\nu'=0}^{D_{\nu}-1} \alpha_{\tilde{\nu}\nu'}^* \gamma_{\nu'r} |\tilde{\nu}\rangle |r\rangle \\ &= \sum_{r=0}^{D_r-1} \sum_{\tilde{\nu}=0}^{D_{\tilde{\nu}}-1} \sum_{\nu,\nu'=0}^{D_{\nu}-1} \alpha_{\tilde{\nu}\nu} \alpha_{\tilde{\nu}\nu'}^* \gamma_{\nu'r} |\nu\rangle |r\rangle. \end{aligned} \quad (6)$$

We call $\{|\tilde{\nu}\rangle\}$ an optimized basis, if $|\tilde{\psi}\rangle$ is as close as possible to the original state $|\psi\rangle$. Therefore we minimize $\| |\psi\rangle - |\tilde{\psi}\rangle \|^2$ with respect to the elements $\alpha_{\tilde{\nu}\nu}$ of the transformation matrix α under the orthogonality condition $\langle \tilde{\nu}' | \tilde{\nu} \rangle = \sum_{\nu=0}^{D_{\nu}-1} \alpha_{\tilde{\nu}'\nu}^* \alpha_{\tilde{\nu}\nu} = \delta_{\tilde{\nu}'\tilde{\nu}}$. Applying the latter condition, we find

$$\begin{aligned} \| |\psi\rangle - |\tilde{\psi}\rangle \|^2 &= \langle \psi | \psi \rangle - \langle \tilde{\psi} | \psi \rangle - \langle \psi | \tilde{\psi} \rangle + \langle \tilde{\psi} | \tilde{\psi} \rangle \\ &= 1 - \left[\sum_{r=0}^{D_r-1} \sum_{\tilde{\nu}=0}^{D_{\tilde{\nu}}-1} \sum_{\nu,\nu'=0}^{D_{\nu}-1} \gamma_{\nu'r}^* \alpha_{\tilde{\nu}\nu} \alpha_{\tilde{\nu}\nu'}^* \gamma_{\nu'r} + \text{H.c.} \right] \\ &\quad + \sum_{r=0}^{D_r-1} \sum_{\tilde{\nu},\tilde{\nu}'=0}^{D_{\tilde{\nu}}-1} \sum_{\nu,\nu',\nu''=0}^{D_{\nu}-1} \gamma_{\nu''r}^* \alpha_{\tilde{\nu}'\nu''} \alpha_{\tilde{\nu}\nu}^* \alpha_{\tilde{\nu}\nu'} \alpha_{\tilde{\nu}\nu''}^* \gamma_{\nu'r} \\ &= 1 - \sum_{r=0}^{D_r-1} \sum_{\tilde{\nu}=0}^{D_{\tilde{\nu}}-1} \sum_{\nu,\nu'=0}^{D_{\nu}-1} \alpha_{\tilde{\nu}\nu} \gamma_{\nu'r}^* \gamma_{\nu'r} \alpha_{\tilde{\nu}\nu'}^* \\ &= 1 - \text{Tr}(\alpha \rho \alpha^\dagger), \end{aligned} \quad (7)$$

where $\rho = \sum_{r=0}^{D_r-1} \gamma_{\nu'r}^* \gamma_{\nu'r}$ is called the *density matrix* of the state $|\psi\rangle$ with respect to $\{|\nu\rangle\}$. We observe immediately that the states $\{|\tilde{\nu}\rangle\}$ are optimal if the rows of α are eigenvectors of ρ corresponding to its $D_{\tilde{\nu}}$ largest eigenvalues $w_{\tilde{\nu}}$.

Following Zhang et al. [14], we now apply these features to construct an optimized phonon basis for the eigenstates of an interacting electron/spin-phonon system. Consider a system composed of N sites, each contributing a phonon degree of freedom $|\nu_i\rangle$, $\nu_i = 0 \dots \infty$, and some other (spin or electronic) states $|r_i\rangle$. Hence, the Hilbert space of the model under consideration is spanned by the basis $\{ \bigotimes_{i=0}^{N-1} |\nu_i\rangle |r_i\rangle \}$. Of course, to numerically diagonalize an Hamiltonian operating on this space, we need to restrict ourselves to a finite-dimensional subspace. To calculate, for instance, the lowest eigenstates of the HHM (1)-(3) we could limit the phonon space spanned by $|\nu_i\rangle = (\nu_i!)^{-1/2} (b_i^\dagger)^{\nu_i} |0\rangle$ by allowing only the states $\nu_i < D_i$. Most simply we can choose $D_i = M \forall i$ yielding $D_{\text{ph}} = M^N$ for the dimension of the total phonon space. However, if we think of the states $\{ \bigotimes_{i=0}^{N-1} |\nu_i\rangle \}$ as eigenstates of the Hamiltonian $\mathcal{H}_{\text{ph}} = \omega \sum_{i=0}^{N-1} b_i^\dagger b_i$, it is more suitable for most problems to choose an energy cut-off instead. Thus we used the condition

$\sum_{i=0}^{N-1} \nu_i < M$, leading to $D_{\text{ph}} = \binom{N+M-1}{N}$, for most of our previous numerical work (see e.g. Ref. [15]). For weakly interacting systems already a small number M of phonon states is sufficient to reach very good convergence for ground states and low-lying excitations. However, with increasing coupling strength most systems require a large number of the above 'bare' phonons, thus exceeding capacities of even large supercomputers. In some cases one can avoid these problems by choosing an appropriate unitary transformation of the Hamiltonian (e.g. by using center-of-mass coordinates), but in general it is desirable to find an optimized basis automatically.

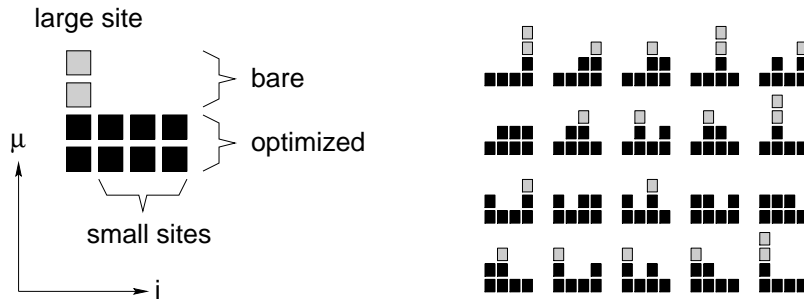


Fig. 1. Structure of the phonon basis in terms of the highest accessible μ_i . Left: as proposed by Zhang et al. [14]; Right: used within this work.

Within the current density-matrix algorithm [14] for the construction of an optimal phonon basis the phonon subsystem is considered as a product of one 'large' ($i = 0$) and a number of 'small' sites ($i > 0$). Each site except the large one uses the same optimized basis $\{|\mu_{i>0}\rangle\} = \{|\tilde{\nu}\rangle\}$ with $\tilde{\nu} = 0 \dots (m-1)$, while the basis of the large site consists of the states $\{|\tilde{\nu}\rangle\}$ plus some bare states $\{|\nu\rangle\}$, $\{|\mu_0\rangle\} = \text{ON}(\{|\tilde{\nu}\rangle\} \cup \{|\nu\rangle\})$, where $\text{ON}(\dots)$ denotes orthonormalization (see Figure 1). After a first initialization the optimized states are improved iteratively through the following steps

- (1) calculating the requested eigenstate $|\psi\rangle$ of the Hamiltonian \mathcal{H} in terms of the actual basis,
- (2) replacing $\{|\tilde{\nu}\rangle\}$ with the most important (i.e., largest eigenvalues $w_{\tilde{\nu}}$) eigenstates of the density matrix ρ , calculated with respect to $|\psi\rangle$ and $\{|\mu_0\rangle\}$,
- (3) changing the additional states $\{|\nu\rangle\}$ in the set $\{|\mu_0\rangle\}$,
- (4) orthonormalizing the set $\{|\mu_0\rangle\}$, and returning to step (1).

A simple way to proceed in step (3) is to sweep the bare states $\{|\nu\rangle\}$ through a sufficiently large part of the infinite dimensional phonon Hilbert space. One can think of the algorithm as 'feeding' the optimized states with bare

phonons, thus allowing the optimized states to become increasingly perfect linear combinations of bare phonon states. Of course the whole procedure converges only for eigenstates of \mathcal{H} at the lower edge of the spectrum, since usually the spectrum of a Hamiltonian involving phonons has no upper bound. The applicability of the algorithm was demonstrated in Ref. [14] with the Holstein model (i.e., $U = 0$ in Eq. (1)) as an example.

When we implemented the above algorithm together with a Lanczos ED method for our systems of interest, we found two objections against the above choice of an optimized basis: (i) the basis is not symmetric under the symmetry operations of the Hamiltonian (e.g. translations), and (ii) the phonon Hilbert space is still large ($D_{\text{ph}} = M m^{N-1}$, where M is the dimension at the large site), since we usually need more than one optimized state per site.

The first problem is solved by including all those states into the phonon basis that can be created by symmetry operations (see Figure 1, right panel), and by calculating the density matrix in a symmetric way, i.e., by adding the density matrices generated with respect to every site, not just site $i = 0$. Concerning the second problem we note that the eigenvalues $w_{\tilde{\nu}}$ of the density matrix ρ decrease approximately exponentially, see Figure 3. If we interpret $w_{\tilde{\nu}} \sim \exp(-a\tilde{\nu})$ as the probability of the system to occupy the corresponding optimized state $|\tilde{\nu}\rangle$, we immediately find that the probability for the complete phonon basis state $\bigotimes_{i=0}^{N-1} |\tilde{\nu}_i\rangle$ is proportional to $\exp(-a \sum_{i=0}^{N-1} \tilde{\nu}_i)$. This is reminiscent of the energy cut-off discussed above, and we therefore propose the following choice of phonon basis states at each site,

$$\forall i : \{|\mu_i\rangle\} = \text{ON}(\{|\mu\rangle\}) \quad (8)$$

$$|\mu\rangle = \begin{cases} \text{opt. state } |\tilde{\nu}\rangle, & 0 \leq \mu < m \\ \text{bare state } |\nu\rangle, & m \leq \mu < M \end{cases}, \quad (9)$$

and for the complete phonon basis $\left\{ \bigotimes_{\Sigma_i \mu_i < M} |\mu_i\rangle \right\}$, yielding $D_{\text{ph}} = \binom{N+M-1}{N}$.

To discuss the nature of the obtained optimized states, the convergence of the algorithm, and some variants in more detail, let us consider a special case of the HHM, Eq. (3), namely the Holstein model of spinless fermions in one dimension,

$$\mathcal{H} = -t \sum_i \left[c_i^\dagger c_{i+1} + \text{H.c.} \right] + g\omega_0 \sum_i (b_i^\dagger + b_i)(n_i - \frac{1}{2}) + \omega_0 \sum_i b_i^\dagger b_i. \quad (10)$$

The optimized phonon approach comes into play in the case of strong electron-phonon coupling g . Then the systems develops lattice distortions which accompany the itinerant fermions. These finite elongations need to be expressed in terms of Harmonic oscillator states $|\nu_i\rangle = (\nu_i!)^{-1/2} (b_i^\dagger)^{\nu_i} |0\rangle$, that are centered around the equilibrium position. Hence, for the numerical diagonalization either a large number of these 'bare' states or some other states embodying a finite distortion are required. By 'sweeping' through the large space of 'bare' phonons, the above optimization procedure automatically creates a

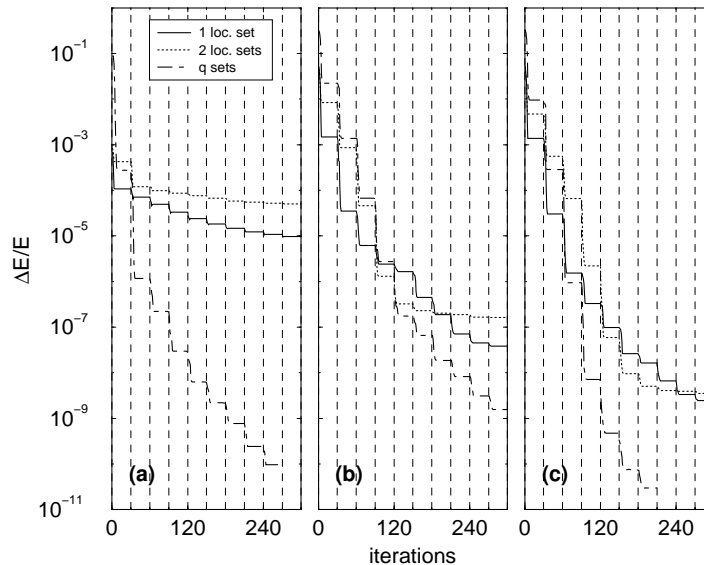


Fig. 2. Convergence of the ground-state energy for the Holstein model, Eq. (10), with electron-phonon coupling $g = 5$ and different phonon frequencies: (a) $\omega_0 = 0.1t$, (b) $\omega_0 = t$, and (c) $\omega_0 = 10t$. Solid lines: one local set, dotted lines: two local sets for each fermion state, dot-dashed lines: momentum dependent sets.

small number of basis states $|\tilde{\nu}\rangle$, which are sufficient for a good approximation of eigenstates of $\mathcal{H}(t, g, \omega_0)$.

In Figure 2 the convergence of the ground state energy of a two-site system at half-filling is shown for an increasing number of iterations (solid lines). We compare the results of an ordinary diagonalization using up to $M = 80$ bare phonons per site (i.e., $D_{\text{ph}} = \binom{N+M-1}{N} = 3240$) and of the optimized approach. In the latter case the phonon basis consists of 6 optimized and 4 bare states, i.e., $M = 10$ and $D_{\text{ph}} = 55$. Each optimized state is chosen to be a linear combination of the first 120 bare states. Initially we set $|\tilde{\nu}\rangle = |\nu\rangle$ and then sweep the 4 bare states through the states $|\nu\rangle$ with $\nu = 0 \dots 119$. Vertical dashed lines denote the end of each sweep. The plateau structure is due to the fact that states of high ν are less important for the optimized basis $|\tilde{\nu}\rangle$. Note that every iteration involves the calculation and diagonalization of the density matrix, an update of the operators $b_i^{(\dagger)}$, which need to be transformed to the current basis, and, most expensive, a Lanczos iteration to obtain a new approximation for the requested eigenstate of \mathcal{H} . It is therefore recommended to use the optimized states obtained for a small cluster as the initial basis

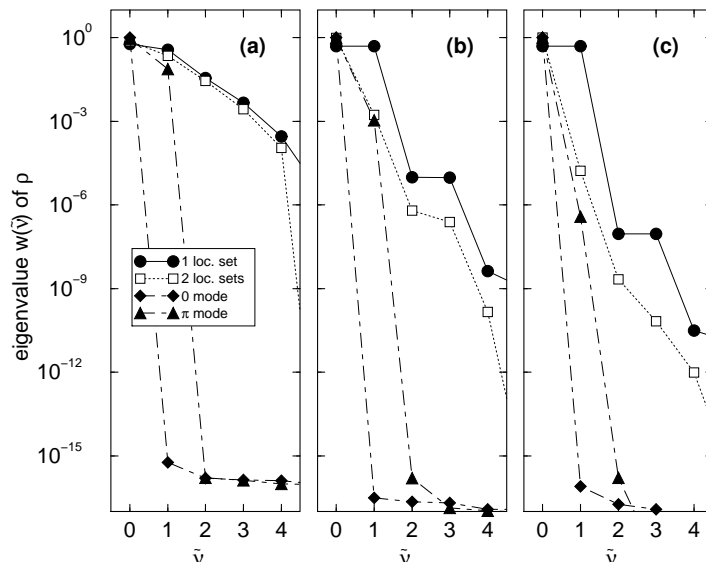


Fig. 3. Eigenvalues $w_{\tilde{\nu}}$ of ρ calculated with the ground state of the Holstein model for $g = 5$ and frequencies: (a) $\omega_0 = 0.1t$, (b) $\omega_0 = t$, and (c) $\omega_0 = 10t$. Filled circles: one local set; open squares: two local sets for each fermion state; filled diamonds and triangles: momentum dependent sets.

for a larger cluster, and to restart the Lanczos procedure with the previous eigenvector (although it is expressed in a slightly different basis).

The figure also includes data for two variants of the algorithm, namely the construction of *two* sets of optimized states, one for each local fermion state, or a transfer of the calculation into *momentum space* and the use of different optimized states for each momentum q . The advantages of these ideas become clear looking at Figure 3. Here the eigenvalues $w_{\tilde{\nu}}$ of the density matrix ρ are given for different phonon frequencies ω_0 and coupling $g = 5$. In the anti-adiabatic regime of high frequencies we observe pairs of equally important eigenstates of ρ [filled circles in panels (b) and (c)]. This indicates that the lattice follows the fermion immediately (small polaron). It is locally distorted to one side or the other, if the site is occupied by an electron or not. Hence, only half of the optimized states couple to one of the local fermion states, and it appears reasonable to use different basis sets for the two situations. This results in step free exponential decrease of the eigenvalues of the density matrices for both basis sets (open squares in Figure 3), which allows for a smaller cut-off M in the total phonon space of the cluster.

However, at small frequencies the lattice is slow compared to the fermions, and distortions are long ranged. Obviously, there is no gain using different

local basis sets, the convergence as well as the decay of the eigenvalues $w_{\tilde{\nu}}$ of the density matrix is slow (see panel (a) in Figures 2 and 3). The performance of each *local* optimization seems to be poor and switching to momentum space is recommended. After a shift of operators, $b_i^{(\dagger)} \rightarrow b_i^{(\dagger)} + \frac{g}{2}$, and Fourier transform the Hamiltonian \mathcal{H} , Eq. (10), reads

$$\begin{aligned} \mathcal{H} &= -t \sum_i \left[c_i^\dagger c_{i+1} + \text{H.c.} \right] + g\omega_0 \sum_i (b_i^\dagger + b_i) n_i + \omega_0 \sum_i b_i^\dagger b_i + E_s \quad (11) \\ &= -2t \sum_k \cos \left[\frac{2\pi}{N} k \right] n_k + \frac{g\omega_0}{\sqrt{N}} \sum_{k,q} (b_{-k}^\dagger + b_k) c_{q+k}^\dagger c_q + \omega_0 \sum_k b_k^\dagger b_k + E_s, \end{aligned}$$

with $E_s = g^2\omega_0 \left(\sum_k n_k - \frac{N}{4} \right)$. Using the same cut-off in the total phonon basis as described before, we now optimize each q -mode separately. The results turn out to be excellent for *all* phonon frequencies. The ground-state energy converges quickly (dot-dashed lines in Figure 2) and only a few optimized states are required, as can be seen from the rapidly decreasing eigenvalues of the density matrix (filled diamonds and triangles in Figure 3).

For illustration, in Figure 4 we give optimal wave functions obtained for the frequencies $\omega_0 = 0.1t$ and $10t$ with $\tilde{\nu}$ increasing from top to bottom. In the left panels bold lines denote the wave functions of a single local set, whereas solid and dashed lines mark the two sets of functions that depend on the fermion occupation number. The right panels show optimal wave functions in momentum space. In all cases x denotes the normalized elongation $\frac{1}{\sqrt{2}}(b^\dagger + b)$, i.e., the expansion of the optimized states $|\tilde{\nu}\rangle = \sum_\nu \alpha_{\tilde{\nu}\nu} |\nu\rangle$ is plotted using Harmonic oscillator eigenfunctions in elongation space,

$$|\nu\rangle = \frac{e^{-x^2/2}}{\sqrt{2^\nu \nu! \sqrt{\pi}}} H_\nu(x), \quad (12)$$

with Hermite polynomials $H_\nu(x)$. In momentum space only one or two states have a non-negligible eigenvalue $w_{\tilde{\nu}}$, therefore higher optimized states, which do not contribute to the ground state of \mathcal{H} , are not expected to be converged. In all cases the most important states ($\tilde{\nu} = 0$) resemble the eigenstates of shifted Harmonic oscillators. If we use a single local set, the states correspond to symmetric and anti-symmetric combinations of left- and right-shifted oscillator functions (remember the step structure in Figure 3). For $\omega_0 = 0.1t$ the shift of the real space functions decreases with higher $\tilde{\nu}$. This reflects the fact, that the lattice is slow and fermions move within a distortion. In comparison, the case of high phonon frequency $\omega_0 = 10t$ is much simpler, as we deal only with states of almost fixed shift.

In summary, the simple example of the two-site Holstein model provides good insight into the properties of the optimized phonon approach. It is very efficient for determining an optimal basis within a given phonon Hilbert space. Nevertheless, we are not relieved from choosing the most appropriate decomposition of our model under consideration. Here physical intuition

and some knowledge of the model is necessary to decide between real and momentum space, or other special choices for the phonon Hilbert space. As demonstrated above, the structure of the optimized wave functions and the behaviour of the eigenvalues of the density matrix may give some hints.

3 Bipolaron band formation in the EHHM

Besides bi-/polaron formation itself, the question of whether polarons or bipolarons can move itinerantly has been the subject of much controversy over the last decades (see, e.g., the debate in Ref. [16]). The existence of polaronic bands has been verified by ED techniques in 1D and 2D [17,18,10], however, since both the width and the (electronic) spectral weight of the polaronic bands are exponentially reduced in the strong-coupling case [19], the coherent band motion of small bi-/polarons becomes rapidly destroyed, e.g. by impurities or thermal fluctuations.

Recently it has been discovered that a longer-range EP interaction leads to a decrease in the effective mass of polarons [3,4] and bipolarons [5] in the strong-coupling regime, which can have significant consequences because the quasi-particles are more likely to remain mobile. Indeed, for the single-electron extended Holstein model (1) the polaron band dispersion was shown to be less renormalized as compared to the Holstein model [4]. Here we would like to present some results for the two-electron case, where the competition between attractive EP interaction and Coulomb repulsion becomes important.

By applying the optimized phonon approach outlined in Sec. 2 to EHHM we obtain the lowest eigenvalues of the two-particle system in each K sector ($E_2(K)$), presented in Fig. 5. The gain in performance compared to ordinary ED is illustrated in Table 1. The EP parameters $\varepsilon_p/t = 3.0$ and $\omega_0/t = 0.5$ are chosen in order to address the intermediate coupling and frequency regime, which is almost impossible to investigate analytically. At

	phonon cut-off	matrix dimension	Lanczos diagonalizations	memory requirement	CPU time per run
ED	$M = 81$	$\sim 5 \times 10^{13}$	1	$\gg 1000$ TBytes	???
optimized phonons	$M = 13$ $m = 7$	1.8×10^6	50-300	~ 500 MBytes	$\sim 20 - 200$ CRAY T3E hrs

Table 1. Problem sizes and computer requirements for the exact diagonalization method (ED) and the optimized phonon approach to solve one parameter set of the bipolaron problem on a ten-site lattice within the same accuracy. For both strategies the calculation of the ground-state in a fixed K -sector is assumed.

first we note that the two electrons always form a bipolaronic bound state in the EHHM: The bipolaron binding energy $\Delta = E_2(0) - 2E_1(0)$ is negative, *irrespective* of the Hubbard interaction strength U (see inset of Fig. 5). This is an important difference between the EHHM and the HHM. In the HHM, a critical interaction U_c exists for any EP coupling where the bipolaron unbinds [5,20,21]. Then, calculating the K -dependent binding energy, defined as $\Delta(K) = E_2(K) - \min_{K', K''} [E_1(K') + E_1(K'')]$ with $K' + K'' = K \pmod{2\pi}$, we find a bound bipolaron for *all* K -values. This means that the dispersion curves depicted in Fig. 5 can be deemed to be well-defined bipolaron quasiparticle bands. Of course, due to the “dressing” with phonons, the effective mass of the bipolaron is substantially enhanced. Accordingly the coherent bandwidth of the EHHM bipolaron, $\Delta E = E_2(\pi) - E_2(0)$, is reduced as compared to the free electron case but, on the other hand, it is notably larger than those of the HHM bipolaron, indicating that the EHHM bipolaron is a rather mobile quasiparticle. As U increases ΔE monotonously decreases, which clearly is a correlation effect (put in mind that U hinders double occupancy). At last we notice that the band structure of the bipolaron significantly deviates from a rescaled cosine band only for U much smaller than $2\tilde{\varepsilon}_p$. In this case the on-site and nearest-neighbour density-density correlation functions are about the same size. For $U \gtrsim 2\tilde{\varepsilon}_p$ the band becomes almost cosine shaped. This striking cosine band dispersion, indicating free-particle like behaviour, was previously observed for the HHM model near $U = 2\varepsilon_p$ (Refs. [18,21], cf. also open symbols in Fig. 5), and has been attributed to the formation of an *inter-site bipolaron*. If the inter-site bipolaron moves as a bound pair through the lattice, owing to the retardation effect ($\omega_0 < t$), the second electron can take the advantage of the lattice distortion left by the first one, still avoiding the on-site Coulomb repulsion. As a result the residual bipolaron-phonon interaction is small.

To gain more insight into the differences between EHHM and HHM bipolaronic states, we have calculated the bipolaron kinetic energy, E_{kin} , given by the ground-state average of the first term of (1). Figure 6 presents E_{kin} as a function of the EP interaction parameter ε_p at fixed $U/t = 6$ and $\omega_0/t = 0.5$. Comparing the results for the EHHM and HHM, we can distinguish three regimes. For small EP couplings, the two polarons are bound in the EHHM, but not in the HHM. The higher kinetic energy of the EHHM bipolaron is mainly due to the larger incoherent contribution to the f-sum rule, which originates from incoherent hopping processes of the two charge carriers within the joint lattice distortion spread over the whole lattice. In the intermediate coupling regime predominantly inter-site bipolarons are formed in both models. Now the coherent part to the f-sum rule being proportional to the (inverse) effective mass) plays a decisive role. The EHHM bipolaron has to drag a larger phonon cloud than the HHM bipolaron coherently through the lattice and therefore acquires a larger effective mass. At strong EP couplings, in the HHM, a second transition to an on-site bipolaronic state takes place at about $\varepsilon_p/t = 3 (\simeq U/2)$, whereas the EHHM bipolaron stays in a spatially

much more extended state. Consequently we observe a very gradual decrease of the bipolaron kinetic energy for the EHHM. Finally we comment on the renormalization of the coherent bandwidth of the EHHM bipolaron. As in the single polaron case, at small EP couplings the band structure is flattened near the zone boundary by the intersection with the dispersionsless phonon branch. Hence we find $\Delta E \simeq 0.5$ for $\varepsilon_p/t \ll 1$. The strong reduction of the bandwidth starting to come in at about $\varepsilon_p/t \gtrsim 1$ can be traced back to the formation of a bipolaron with pronounced nearest-neighbour correlations.

4 Summary

The objective of this work was the presentation of an advanced phonon optimization algorithm for application in Lanczos diagonalizations. At the heart of our procedure an 'optimized' phonon basis is created automatically, improving the most important eigenstates of the density matrix by means of gradual 'sweeps' through a sufficiently large part of the infinite dimensional phonon Hilbert space. Within this scheme the density matrix is calculated in compliance with the symmetries of the underlying model. Depending on the physical problem under consideration, the efficiency of the proposed method might be improved considerably using more than one set of optimized phonon states or by performing the optimization procedure in momentum space.

The reliability of our approach was demonstrated by calculating the band dispersion of bipolarons in the framework of the extended Holstein Hubbard model. In comparison with the Holstein Hubbard model where with increasing strength of the EP interaction a sequence of transitions from two unbound large polarons to an inter-site bipolaron and finally to a self-trapped on-site bipolaron takes place, in the EHHM the two electrons form a bipolaronic bound state for all EP couplings, irrespective of the magnitude of the Hubbard interaction. As an effect of the longer ranged non-screened EP coupling included in the EHHM, the EHHM bipolaron is a rather mobile spatially extended quasiparticle even in the extreme strong-coupling regime.

References

1. S. Jin, T. H. Tiefel, M. McCormack, R. A. Fastnach, R. Ramesh, and L. H. Chen, *Science* **264**, 413 (1994).
2. J. Nagamatsu, N. Nakagawa, T. Muranaka, Y. Zenitani, and J. Akimitsu, *Nature* **410**, 63 (2001).
3. A. S. Alexandrov and P. E. Kornilovitch, *Phys. Rev. Lett.* **82**, 807 (1999).
4. H. Fehske, J. Loos, and G. Wellein, *Phys. Rev. B* **61**, 8016 (2000).
5. J. Bonča and S. A. Trugman, arXiv:cond-mat/0103457 (2001).
6. H. Fröhlich, *Adv. Phys.* **3**, 325 (1954).
7. T. Holstein, *Ann. Phys.* **8**, 325 (1959).
8. J. Ranninger and U. Thibblin, *Phys. Rev. B* **45**, 7730 (1992).

9. A. S. Alexandrov, V. V. Kabanov, and D. K. Ray, Phys. Rev. B **49**, 9915 (1994).
10. G. Wellein and H. Fehske, Phys. Rev. B **56**, 4513 (1997).
11. H. D. Raedt and A. Lagendijk, Phys. Rev. Lett. **49**, 1522 (1982).
12. E. Berger, P. Valášek, and W. v. d. Linden, Phys. Rev. B **52**, 4806 (1995).
13. S. R. White, Phys. Rev. B **48**, 1993 (1993).
14. C. Zhang, E. Jeckelmann, and S. R. White, Phys. Rev. Lett. **60**, 2661 (1998).
15. B. Bäuml, G. Wellein, and H. Fehske, Phys. Rev. B **58**, 3663 (1998).
16. Y. Bar-Yam, T. Egami, J. M. de Leon, and A. R. Bishop, *Lattice Effects in High- T_c Superconductors*, World Scientific, (Singapore 1992).
17. W. Stephan, Phys. Rev. B **54**, 8981 (1996).
18. G. Wellein, H. Röder, and H. Fehske, Phys. Rev. B **53**, 9666 (1996).
19. H. Fehske, J. Loos, and G. Wellein, Z. Phys. B **104**, 619 (1997).
20. J. Bonča, T. Kataršnik, and S. A. Trugman, Phys. Rev. Lett. **84**, 3153 (2000).
21. A. Weiße, H. Fehske, G. Wellein, and A. R. Bishop, Phys. Rev. B **62**, R747 (2000).

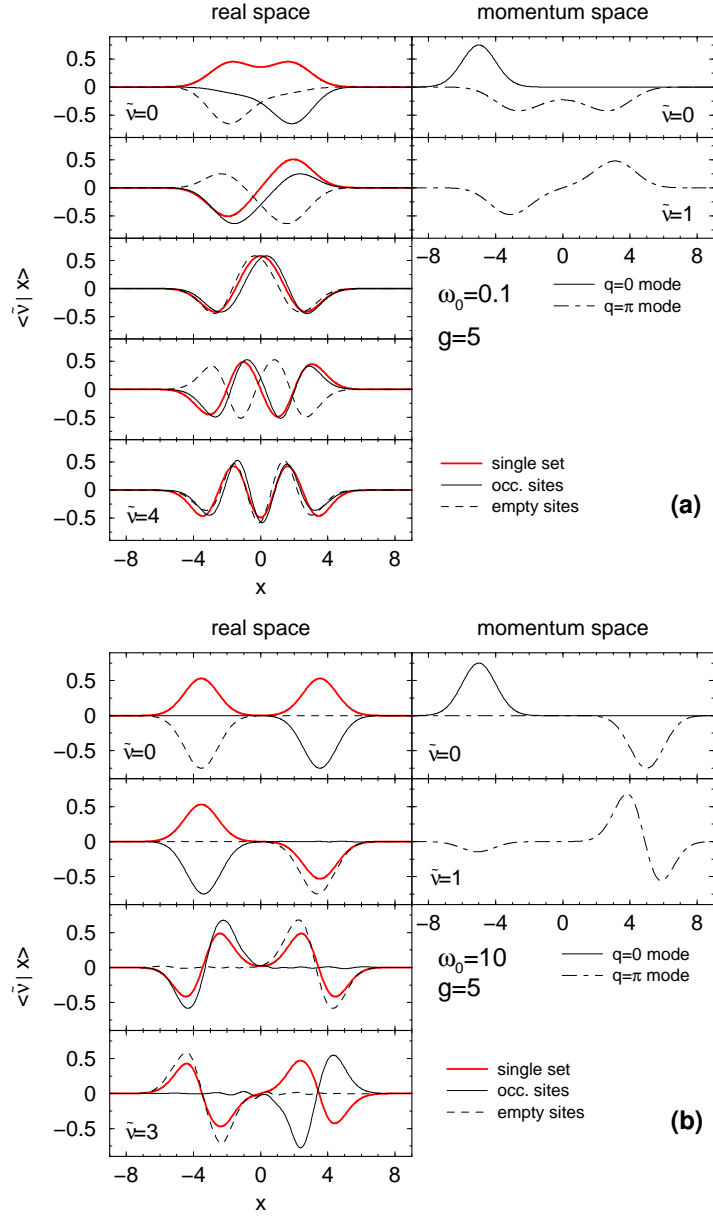


Fig. 4. Optimized phonon states in elongation space for (a) $\omega_0 = 0.1 t$, and (b) $\omega_0 = 10 t$, and different choices of the optimized basis (left panels: real space; right panels: momentum space).

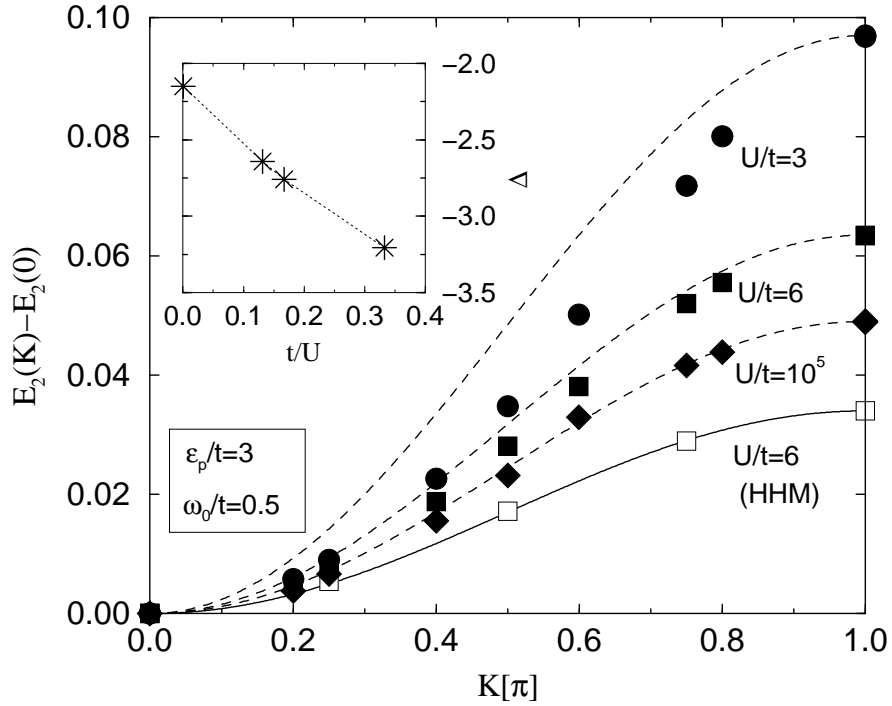


Fig. 5. Bipolaron band structure in the 1D extended Holstein Hubbard model. Data points (filled symbols) are obtained from exact diagonalizations of the EHHM on eight- and ten-site chains (employing periodic boundary conditions) with different Hubbard interaction strengths; dotted lines give the corresponding rescaled cosine bands having the same bandwidths. At $U/t = 6$, the bipolaron band dispersion of the Holstein Hubbard model is included for comparison (open symbols). The inset displays the bipolaron binding energy Δ as a function of the inverse Hubbard interaction strength.

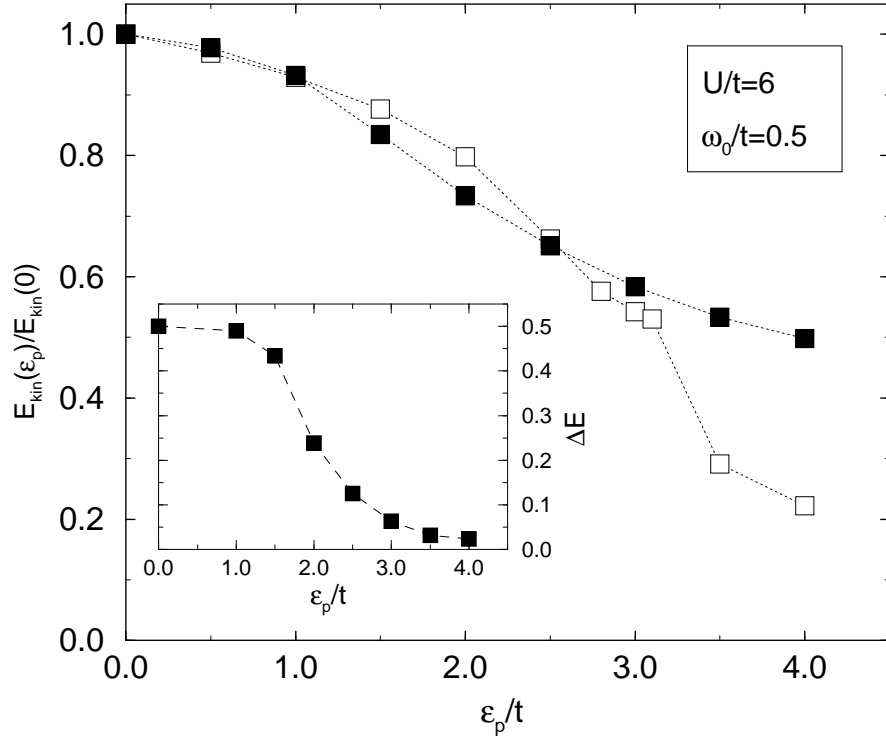


Fig. 6. Renormalized bipolaron kinetic energy in the eight-site EHHM (filled symbols) and HHM (open symbols). The inset gives the coherent bandwidth of the bipolaron in dependence on the EP coupling strength.